Am. J. Hum. Genet. 68:711–722, 2001

A Phase 1/2 Clinical Trial of Enzyme Replacement in Fabry Disease: Pharmacokinetic, Substrate Clearance, and Safety Studies

Christine M. Eng,[1,*] Maryam Banikazemi,[1] Ronald E. Gordon,[2] Martin Goldman,[3] Robert Phelps,[4] Leona Kim,[3] Alan Gass,[3] Jonathan Winston,[3] Steven Dikman,[2] John T. Fallon,[2,3] Scott Brodie,[5] Charles B. Stacy,[6] Davendra Mehta,[3] Rosaleen Parsons,[7] Karen Norton,[7] Michael O'Callaghan,[8] and Robert J. Desnick[1]

Departments of [1]Human Genetics, [2]Pathology, [3]Medicine, [4]Dermatology, [5]Ophthalmology, [6]Neurology, and [7]Radiology, Mount Sinai School of Medicine, New York, and [8]Genzyme Corporation, Cambridge, MA

Fabry disease results from deficient α-galactosidase A (α-Gal A) activity and the pathologic accumulation of the globotriaosylceramide (GL-3) and related glycosphingolipids, primarily in vascular endothelial lysosomes. Treatment is currently palliative, and affected patients generally die in their 40s or 50s. Preclinical studies of recombinant human α-Gal A (r-hαGalA) infusions in knockout mice demonstrated reduction of GL-3 in tissues and plasma, providing rationale for a phase 1/2 clinical trial. Here, we report a single-center, open-label, dose-ranging study of r-hαGalA treatment in 15 patients, each of whom received five infusions at one of five dose regimens. Intravenously administered r-hαGalA was cleared from the circulation in a dose-dependent manner, via both saturable and nonsaturable pathways. Rapid and marked reductions in plasma and tissue GL-3 were observed biochemically, histologically, and/or ultrastructurally. Clearance of plasma GL-3 was dose-dependent. In patients with pre- and posttreatment biopsies, mean GL-3 content decreased 84% in liver ($n = 13$), was markedly reduced in kidney in four of five patients, and after five doses was modestly lowered in the endomyocardium of four of seven patients. GL-3 deposits were cleared to near normal or were markedly reduced in the vascular endothelium of liver, skin, heart, and kidney, on the basis of light- and electron-microscopic evaluation. In addition, patients reported less pain, increased ability to sweat, and improved quality-of-life measures. Infusions were well tolerated; four patients experienced mild-to-moderate reactions, suggestive of hypersensitivity, that were managed conservatively. Of 15 patients, 8 (53%) developed IgG antibodies to r-hαGalA; however, the antibodies were not neutralizing, as indicated by unchanged pharmacokinetic values for infusions 1 and 5. This study provides the basis for a phase 3 trial of enzyme-replacement therapy for Fabry disease.

Introduction

Fabry disease (MIM 301500) is an X-linked inborn error of glycosphingolipid catabolism resulting from the deficient activity of the lysosomal exoglycohydrolase, α-galactosidase A (α-Gal A) (Desnick et al. 1995, 2001). In patients with the classical disease phenotype, the progressive accumulation of globotriaosylceramide (GL-3) and related glycosphingolipids, particularly in vascular endothelial lysosomes in the heart, liver, kidney, skin, and brain, leads to the major disease manifestations. Clinical onset occurs in childhood or adolescence and is characterized by severe acroparesthesias, angiokeratoma, corneal and lenticular opacities, and hypohidrosis. With advancing age, renal failure and vascular disease of the heart and brain lead to early demise, the average age at death being 41 years in one series (Colombi et al. 1967). To date, there is no specific therapy for Fabry disease, and treatment is supportive, limited to symptomatic management of the acroparesthesias and episodes of excruciating pain and of complications of renal failure, cardiac, or cerebrovascular disease.

It is of relevance that patients with residual α-Gal A activity (~1% to ~10% of normal) are essentially asymptomatic or have a mild form of the disease limited to cardiac involvement (von Scheidt et al. 1991; Desnick et al. 2001). These "cardiac variants" typically present in late adulthood (>40 years) with left ventricular hypertrophy, cardiomyopathy, and/or mild proteinuria. They lack the classic disease manifestations, which include angiokeratoma, acroparesthesias, hypohidrosis, corneal/lenticular dystrophy, and renal failure. A consistent feature of the cardiac variant is the absence of

Received December 27, 2000; accepted for publication January 12, 2001; electronically published February 1, 2001.

Address for correspondence and reprints: Dr. R. J. Desnick, Professor and Chairman, Department of Human Genetics, Box 1498, Mount Sinai School of Medicine, Fifth Avenue and 100th Street, New York, NY 10029. E-mail: rjdesnick@mssm.edu

* Present affiliation: Department of Molecular and Human Genetics, Baylor College of Medicine, Houston.

0002-9297/2001/6803-0016$02.00

lysosomal glycosphingolipid accumulation in the vascular endothelium (Elleder et al. 1990; von Scheidt et al. 1991), the pathogenic hallmark of classically affected patients (Desnick et al. 2001). The cardiac variants demonstrate that even low levels of α-Gal A activity can markedly alter the classic disease phenotype, particularly the morbidity associated with the progressive vascular endothelial glycosphingolipid deposition.

Early pilot trials of enzyme replacement in classically affected males involved the intravenous administration of either a single dose of fresh normal plasma containing active α-Gal A (Mapes et al. 1970) or a single dose of the partially purified placental enzyme (Brady et al. 1973). These studies demonstrated that intravenously infused enzyme from plasma or placenta could decrease the level of accumulated plasma GL-3. In a subsequent study, two affected brothers each received six doses of α-Gal A purified from splenic tissue or plasma over a 3-mo period (Desnick et al. 1979). The splenic-derived enzyme was cleared rapidly from the circulation ($t_{1/2}$ ~10 min), transiently decreasing the circulating GL-3 concentration, whereas the more highly sialylated plasma-derived enzyme had a slower clearance ($t_{1/2}$ ~70 min) and effected a longer depletion of circulating GL-3. Notably, two doses of the plasma-derived enzyme, administered on days 1 and 3, reduced the plasma substrate level into the normal range (Desnick et al. 1980). These studies demonstrated the feasibility of enzyme-replacement therapy for Fabry disease; however, the difficulty of producing enough purified enzyme for clinical trials was a major obstacle.

This obstacle was overcome following the isolation of the human α-Gal A cDNA (Bishop et al. 1986) and demonstration of its high-level expression in Chinese hamster ovary (CHO) cells (Ioannou et al. 1992), thereby providing a source of both lysosomal (oligosaccharide processed) and secreted (highly-sialylated) glycoforms of the enzyme (Matsuura et al. 1998). In addition, the generation of knockout "Fabry mice" with α-Gal A deficiency (Wang et al. 1996) permitted determination, by preclinical studies, of the pharmacokinetics and biodistributions of various recombinant human α-Gal A (r-hαGalA) glycoforms (Ioannou et al. 2001). When a highly sialylated glycoform (AGA-1) was used, these animal-model studies demonstrated a dose-dependent clearance of accumulated GL-3 from the circulation and from the pathologic sites of substrate deposition in the liver, heart, kidney, and skin (Ioannou et al. 2001), thereby establishing "proof of concept" for clinical trials of r-hαGalA replacement in patients with Fabry disease. In addition, in a recent phase 1 study, single doses of recombinant enzyme reduced GL-3 levels in liver and urinary sediment (Schiffmann et al. 2000).

Here, we report the results of a phase 1/2 trial of five dose regimens of r-hαGal A in 15 classically affected males with Fabry disease. This open-label dose-escalation study was conducted to evaluate the safety and pharmacokinetics of r-hαGalA infusions and to provide preliminary efficacy data for enzyme-replacement therapy in this lysosomal-storage disease.

Material and Methods

Study Design

Fifteen classically affected male patients with Fabry disease were recruited for this multidose, open-label, single-center, dose-escalation study of r-hαGalA (Fabrazyme [agalsidase beta]; Genzyme). Participants were aged ⩾16 years and had α-Gal A activity in plasma <1.5 nmol/h/ml, GL-3 concentrations in plasma ⩾5.0 ng/μl, serum creatinine <2.5 mg/dl, and no history of renal dialysis or transplantation. Patients were sequentially enrolled into one of five r-hαGalA dosing regimens with three patients per group. The characteristics of the five groups are shown in table 1. Patients in each group received five doses of enzyme as follows: Group A, 0.3 mg/kg of r-hαGalA every 14 d (biweekly); Group B, 1.0 mg/kg biweekly; Group C, 3.0 mg/kg biweekly; Group D, 1.0 mg/kg every 48 h; and Group E, 3.0 mg/kg every 48 h. R-hαGalA was synthesized in CHO cells, and the secreted homodimeric enzyme was purified from the growth medium. Each enzyme subunit contained three glycosylation sites, with the predominant oligosaccharides being bi- and monophosphorylated oligomannose structures and sialylated complex structures. Enzyme was diluted to 100 ml with saline, and infusions were given intravenously at a rate of 0.83 ml/min. The institutional review board of the Mount Sinai School of Medicine approved the study, and all patients gave written informed consent to participate in the study.

Clinical Assessments

Medical and safety evaluations—including medical history, physical examinations, vital signs, routine serum and urine chemistries, hematology indices, and EKGs—were performed at baseline, prior to each infusion, and after infusion 5. In addition, echocardi-

Table 1

Summary of Patient Demographics

Dose Regimen	Mean Age (Range) (years)	Mean Weight (Range) (kg)	Race (*n*)	
			White	Hispanic
0.3 mg/kg/14 d	41.0 (35–44)	64.7 (57–71)	3	0
1.0 mg/kg/14 d	33.7 (27–38)	73.6 (57–88)	1	2
3.0 mg/kg/14 d	34.7 (32–37)	69.1 (56–82)	2	1
1.0 mg/kg/48 h	27.0 (18–37)	69.8 (65–73)	2	1
3.0 mg/kg/48 h	35.7 (30–45)	78.0 (67–93)	3	0

ograms and renal magnetic resonance imaging (MRI) were evaluated at baseline and after infusion 5. Patients completed the Short Form McGill Pain Survey (Melzack 1987) and the Short Form–36 (SF-36) Health Survey (Ware et al. 1997) to assess quality-of-life measures at baseline and after infusion 5. Patients continued their usual prophylactic and analgesic pain medications. Adverse events were coded using the World Health Organization Adverse Reactions Thesaurus (WHOART). At baseline, prior to each infusion, and after infusion 5, an enzyme-linked immunosorbent assay (ELISA), specific for r-hαGalA, and a confirmatory radioimmunoprecipitation technique were used to assess antibody response to r-hαGalA.

Molecular and Biochemical Studies

Specific mutations in the α-Gal A gene in each patient were previously determined (e.g., Eng et al. 1993). Plasma and tissue α-Gal A activities were measured using 2.5 mM 4-methyumbelliferyl-α-*D*-galactoside as substrate (Desnick et al. 1973). Plasma and tissue GL-3 concentrations were measured using a verotoxin-based ELISA specific for GL-3 (Zeidner et al. 1999). Plasma GL-3 levels were measured at baseline, before each infusion, and either 14 d (for the every-48-h groups) or 21–28 d (for the biweekly groups) after infusion 5.

Collection of Tissue Samples

Percutaneous needle biopsies of liver and 3-mm punch biopsies of skin from the lower back (avoiding angiokeratomas) were collected from all patients at baseline and 2–3 d after infusions 1 and 5. Pre- and posttreatment right-ventricular endomyocardial and kidney biopsies were optional procedures for a subset of participants in groups C, D, and E only. Tissue samples were divided and then prepared for light and electron microscopy or frozen at -80°C for biochemical analyses.

Pharmacokinetic Analyses

For infusions 1 and 5, r-hαGalA activity was determined from blood samples collected at 30, 60, and 90 min during the infusions and at multiple time points 0–480 min after these infusions. These data were evaluated using standard noncompartmental analysis. In addition, concentration-time data were subjected to model-independent pharmacokinetic analysis. The following pharmacokinetic values were determined: (1) area under the curve ($AUC_{0-\infty}$), as computed by the linear trapezoidal rule; (2) area under the moment ($AUMC_{0-\infty}$); (3) peak α-Gal A concentration (C_{max}); (4) time to peak activity (T_{max}); (5) the terminal elimination half-life ($t_{1/2}$); (6) volume of distribution at steady state (VSS); (7) clearance; (8) mean residence time extrapolated to infinity (MRT_{∞}); and (9) the elimination-rate constant (λ_Z).

Histological Evaluations

For light microscopy, tissue was embedded in paraffin (liver, kidney, and skin), glycomethacrylate (kidney), or Epon (skin and heart). Sections were stained with hematoxylin and eosin (liver, kidney), periodic acid-Schiff (liver, skin, and kidney), methylene blue/azure II (skin, heart, kidney), and/or oil red O (skin). For electron microscopy, gluteraldehyde-fixed tissue was posttreated with OsO_4, was epoxy-embedded, was sectioned (4–5 μm), and was viewed under a JOEL transmission electron microscope. Representative tissue specimens were photographed. Scoring of tissue response to treatment was performed with coded instruments designed by expert pathologists for light- and electron-microscopic assessment of the tissue and cell types with significant GL-3 accumulation. Quantitation of GL-3 content for both light and electron microscopy was based on a 4-point scoring system to evaluate the degree and extent of glycosphingolipid inclusions (ranging from 0, normal or near normal, to 3, severe involvement). This system was applied to several structures in each tissue. Exceptions to this format were an extended coding range for the vascular endothelium of the skin (0–5) to account for any accidental inclusion of angiokeratomatous vessels in the biopsy, and a histomorphometric method applied to the tightly grouped inclusions in cardiomyocytes with scores expressed as the volume of inclusions relative to the total volume of tissue evaluated.

Statistical Analyses

Statistical analyses were performed using the Statistical Software System (SAS Institute). The SF-36 questionnaire was analyzed using the SF-36 health scoring system (Ware et al. 1997). A Wilcoxan signed rank test was used to calculate change from baseline for quality of life and pain (Short Form McGill Pain Questionnaire) values (Melzack 1987).

Results

Pharmacokinetics

Concentration-time data for r-hαGalA infusions demonstrated a dose-dependent (nonlinear) profile consistent with enzyme clearance from the circulation via both saturable and nonsaturable (concentration-independent) pathways. Semilog plots of mean concentration-time data for the first 2 h of infusion of r-hαGalA at doses of 0.3, 1.0, or 3.0 mg/kg biweekly (groups A–C) are shown in figure 1. Mean plasma concentrations reached 80% of peak values 60 min into the infusion for the 0.3 mg/kg dose (group A) and 90 min into the infusion for

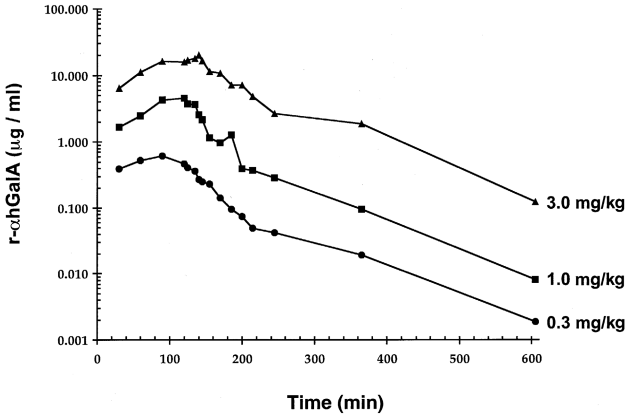

Figure 1 Pharmacokinetics of r-hαGalA infusions. Semilog plots of mean concentration-time data for r-hαGalA infusions at doses of 0.3 (♦), 1.0 (●), or 3.0 (▲) mg/kg (groups A–C), demonstrating the dose-dependent (nonlinear) profile consistent with enzyme cleared from the circulation via both saturable and nonsaturable (concentration independent) pathways. R-hαGalA was infused over 120 min. See text for details.

the 1.0 and 3.0 mg/kg doses (groups B and C). When infusions were completed, mean concentrations dropped to half-peak values within 15, 20, and 45 min for the 0.3-, 1.0-, and 3.0-mg/kg dose groups, respectively. Clearance appeared to be biphasic for all biweekly dose groups, with the more rapid elimination phase lasting 1–2 h after infusion. AUC values were increased disproportionately with dose, from ~80 to ~500 to ~4000 μg/min/ml. The mean VSS had a range of 80–330 ml/kg (1–4 times blood volume). Clearance decreased from 4 ml/min/kg to ~1 ml/min/kg with increasing dose. Of note, the terminal elimination half-life was not affected by dose, which is consistent with elimination being governed, in part, by a first-order, concentration-independent mechanism.

Plasma GL-3 Clearance was Dose-Dependent

Plasma GL-3 concentrations were reduced in a dose-dependent manner for all infusion groups (fig. 2). Prior to treatment, all patients had elevated plasma GL-3 levels, with a range of 2.0–53.9 ng/μl (mean 17.1 ± 12.8 ng/μl; the normal, undetectable level is <1.2 ng/μl). Plasma GL-3 levels in patients receiving r-hαGalA at 0.3 mg/kg biweekly tended to decrease with each dose, reaching their lowest values only at infusion 5. In contrast, plasma GL-3 levels in all three patients receiving r-hαGalA at doses of 3.0 mg/kg biweekly totally cleared after the first infusion and remained undetectable throughout the clinical trial. Two of three patients receiving r-hαGalA at 1.0 mg/kg biweekly demonstrated plasma GL-3 clearance after the first infusion, whereas the third patient's plasma GL-3 level was reduced but never reached undetectable levels. In patients receiving 1.0 or 3.0 mg/kg every other day (groups D and E), the plasma GL-3 levels were lowest at infusion 4; however, the decreases were less than those observed in patients with biweekly dosing schedules (data not shown).

Tissue GL-3 Clearance Was Dose- and Organ-Dependent

Liver.—Hepatic GL-3 concentrations, measured by ELISA, were reduced by an average of 84% in the 13 patients who had pre- and posttreatment liver biopsies. As shown in table 2, GL-3 clearance was particularly consistent and profound (mean clearance 92%) in group C patients, who received 3.0 mg/kg biweekly. However, marked GL-3 reductions were observed in all dose cohorts. Histologic scores from electron-microscopic evaluations based on the 0–3 scale confirmed the positive response to r-hαGalA treatment, with reductions in mean sinusoid endothelial GL-3 accumulation scores from 2.40 ± 0.74 (n = 15) at baseline to 0.5 ± 0.52 (n = 14) after infusion 5. Mean Kupffer cell scores decreased from 2.80 ± 0.56 (n = 15) to 1.07 ± 0.27

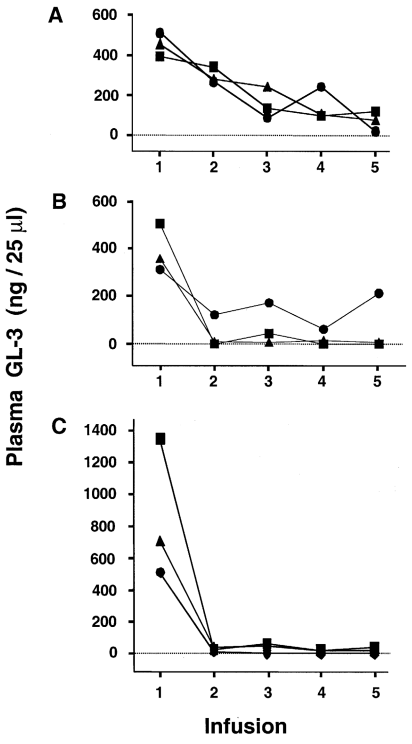

Figure 2 Effect of r-hαGalA dose on plasma GL-3 clearance. Individual patient plasma GL-3 concentrations determined just prior to infusions 1–5 for the 0.3 (*A*), 1.0 (*B*), and 3.0 (*C*) mg/kg biweekly dosing groups.

Table 2

GL-3 Clearance in Liver, Heart and Kidney

Tissue, Dose Regimen, and Patient	Age (years)	α-Gal A Mutation	GL-3 Concentration at Baseline (ng/mg tissue)	GL-3 Concentration 2–5 d after Infusion 5	Reduction (%)
Liver:					
Group A:					
2	44	C56G	870	74	91
3	44	N263S	1,130	48	96
Group B:					
4	27	W287C	832	185	78
5	36	C172Y	176	134	24
6	38	C172Y	2410	45	98
Group C:					
7	32	W226R	371	26	93
8	37	G138E	1,780	153	91
9	35	L89R	352	29	92
Group D:					
10	37	G138E	12,650	5,940	53
11	26	R227Q	1,280	38	97
12	18	W95S	1,640	77	95
Group E:					
13	45	1118 insT	1,690	204	88
15	32	26delA	140	0	100
Heart:					
Group C:					
7	32	W226R	17,600	15,700	11
8	37	G138E	38,100	40,900	−7
9	35	L89R	17,500	12,900	26
Group D:					
10	37	G138E	32,500	29,800	8
11	26	R227Q	17,800	14,800	17
12	18	W95S	8,320	10,700	−29
Group E:					
13	45	1118 insT	25,000	48,100	−93
Kidney:					
Group C:					
8	37	G138E	12,930	384	97
9	35	L89R	6,910	512	93
Group D:					
10	37	G138E	1,060	448	58
11	26	R227Q	10,100	1,980	80
Group E:					
13	45	1118 insT	1,860	5,630	−203

($n = 14$). A dose effect was observed for endothelial GL-3 clearance in dosing cohorts treated biweekly: from baseline, mean scores decreased -1.67 ± 0.58 points for the 0.3-mg/kg group A, -2.00 ± 1.00 points for the 1.0 mg/kg group B, and, -2.33 ± 1.15 points for the 3.0-mg/kg group C. Notably, one patient in Group E had increased sinusoid and Kupffer cell scores and was not included in the histologic analysis.

Skin.—Low and variable GL-3 levels were detected by ELISA in pretreatment skin biopsies (mean 350 ± 168 ng/mg of tissue; range 128–803 ng/mg tissue). Following infusion 5, the mean GL-3 concentration decreased ~40%, to 191 ± 160 ng/mg of tissue. Of the 14 patients with paired samples, 11 had reductions, and 3 (1 from group A and 2 from group D), had increases from baseline.

Pre- and posttreatment skin biopsies were obtained, free of angiokeratomas, for all patients. Histological evaluation resulted in scores of $\leqslant 3$ on the expanded 0–5 scale, except in one patient, who had a baseline capillary endothelial score of 4 (fig. 3*A*). In histologic sections stained with periodic acid-Schiff, markedly reduced mean GL-3 scores were observed in the endothelium of superficial capillaries (from 2.6 ± 0.79 at baseline to

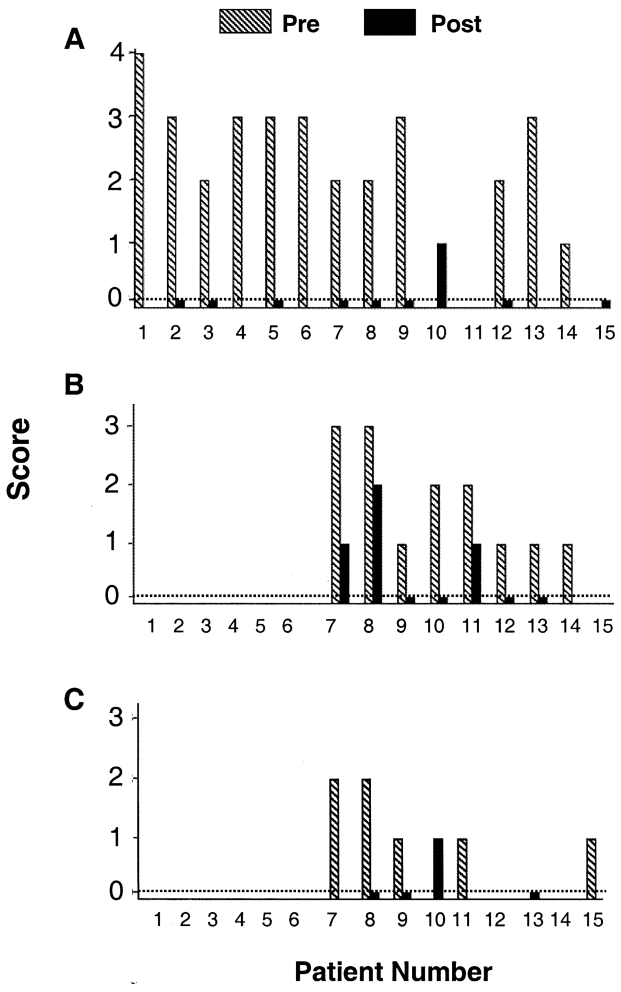

Figure 3 Light-microscopic assessment of the vascular endothelial GL-3 deposits in skin (*A*), heart (*B*), and kidney (*C*), before and after r-hαGalA treatment by expert pathologists blinded to time of biopsy and patient. *A,* Pre- and posttreatment GL-3 scores (ranging from 0, normal or near normal, to 4, severe) of skin capillary endothelium for 14 patients. Note that the seven with paired pre- and posttreatment biopsies all cleared their capillary endothelial GL-3 deposits ("0" scores). *B,* Pre- and posttreatment endomyocardial vascular endothelium GL-3 scores (ranging from 0, normal or near normal, to 3, severe) for seven patients: three in group C, three in group D, and one in group E. Note that the seven patients with paired pre- and posttreatment biopsies all had reduced GL-3 scores and four had cleared their capillary endothelium ("0" scores). *C,* Pre- and posttreatment GL-3 scores (ranging from 0, normal or near normal, to 3, severe) for kidney vascular endothelium for seven patients: three in group C, two in group D, and two in group E. Note that the two with paired pre- and posttreatment biopsies had cleared their capillary endothelial GL-3 deposits ("0" scores). See text for details.

0.11 ± 0.33 after infusion 5), with the greatest improvement in patients in the biweekly dose cohorts. Clearance was observed with all dose regimens, best demonstrated overall by immunohistochemistry (figs. 4*A* and 4*B*). For the perineurium, five of eight patients with paired biopsies showed decreases of 1 or 2 points from baseline. In the deeper arterioles, endothelial scores varied, with three of six patients declining by 1 or 2 points and the others remaining unchanged. Electron-microscopic evaluations provided similar results, with mean scores for GL-3 deposits in endothelial cells of superficial capillaries decreasing from 2.80 ± 0.41 at baseline to 0.50 ± 0.65 after infusion 5. Of 12 patients in treatment groups B–E, 8 essentially cleared all the accumulated GL-3 from the endothelium, achieving scores of 0 after the last infusion (e.g., figs. 4*C* and 4*D*). Similarly, mean GL-3 scores in the endothelium of deeper arterioles showed consistent decreases (3.00 ± 0.0 at baseline to 1.50 ± 1.00; $n = 14$). In contrast, GL-3 deposits in pericytes, perineurium, and the muscular layer of arterioles, as well as the histiocytes and fibrocytes, showed little or no change.

Heart.—Endomyocardial biopsies were obtained pre- and posttreatment in seven patients from groups C, D, and E. As shown in table 2, baseline tissue GL-3 levels, determined by ELISA, were high, with a range of 8,320–38,100 ng/mg tissue (mean 21,400 ± 7,420 ng/mg tissue). Following infusion 5, the mean GL-3 concentration decreased only slightly (15.6%) to 18,300 ± 7,780 ng/mg tissue in four patients with decreases. Histologic scores for the capillary endothelium, assessed by light microscopy (fig. 3*B*), decreased in all seven patients with pre- and posttreatment biopsies; mean scores decreased from 1.75 ± 0.89 at baseline to 0.57 ± 0.79 after treatment. By electron-microscopic examination (e.g., figs. 5*A* and 5*B*), six of seven paired biopsies had decreased scores for vascular endothelial GL-3, whereas one patient's scores remained unchanged (mean scores of 2.14 and 0.71, pre- and posttreatment, respectively). After five infusions, GL-3 storage remained unchanged in the cardiomyocytes, pericytes, and vascular smooth muscle.

Kidney.—Paired pre- and posttreatment kidney biopsies were obtained from five patients: two each in groups C and D, and one in group E. Pretreatment kidney GL-3 concentrations, determined by ELISA, varied considerably (table 2), with a range of 1,060–12,900 ng/mg tissue (mean 5,530 ± 4,580 ng/mg; $n = 5$). Following infusion 5, the mean GL-3 level was decreased by 67.6% to 1,790 ± 2,250 ng/mg in the five patients with paired samples. Four patients decreased their levels by a mean of 84% (mean 830 ± 770 ng/mg), whereas the fifth patient's level almost doubled. Sampling variability may account for part of this discrepancy. Histologic evaluations focused on four functional areas known to harbor prominent GL-3 inclusions: glomeruli, tubules, intertubular interstitium, and larger multilayered vessels. There was a consistent pattern of reduction of GL-3

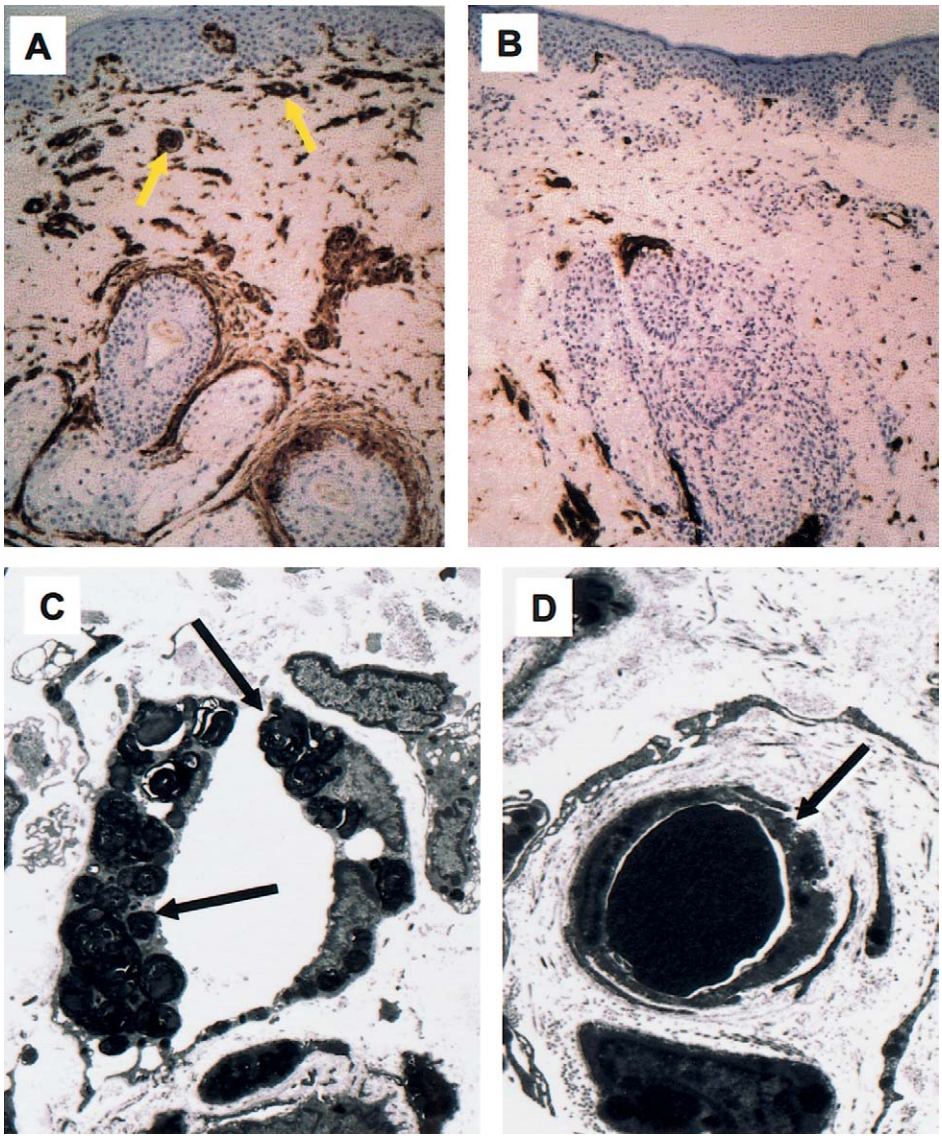

Figure 4 *A* and *B*, Immunohistochemistry for GL-3 in skin with verotoxin subunit B. Comparison of pretreatment (*A*) and posttreatment (*B*) photomicrographs shows that r-hαGalA treatment resulted in marked clearance of GL-3 inclusions, particularly from the superficial vasculature of the papillary dermis. *C* and *D*, Electron micrographs of single superficial capillaries of the skin. Before treatment (*C*), the capillary endothelium was heavily laden with lamellar glycosphingolipid inclusions (*arrows*). After treatment (*D*), the endothelium of superficial capillaries was cleared of GL-3 inclusions (*arrow*). See text for details.

inclusions in the three vascular beds. As shown in figure 3*C*, GL-3 accumulation in the endothelium of interstitial capillaries declined in four of five patients (e.g., fig. 6*A*–6*D*) but increased in one. In two patients with paired glomerular capillary scores, endothelial GL-3 scores declined from 2 to 0 and from 1 to 0, respectively. For the arterioles, four paired samples showed declines in endothelial GL-3 content of $\geqslant 1$ point (mean scores of 2.25 at baseline to 1.00 after treatment).

Response in other tissue types varied considerably. Prominent reductions occurred following treatment in glomerular mesangial cells (from 2.00 at baseline to 0.00 in group C; $n = 2$) and in cortical interstitial cells (2.60 at baseline to 1.00 in groups C, D, and E; $n = 5$). The distal convoluted tubules and collecting ducts that, along with the glomerular podocytes, had the most prominent GL-3 storage in the kidney at baseline were difficult to evaluate but appeared to trend to reduced scores. The glycosphingolipid deposits in the glomerular podocytes appeared unresponsive to treatment. Electron-micro-

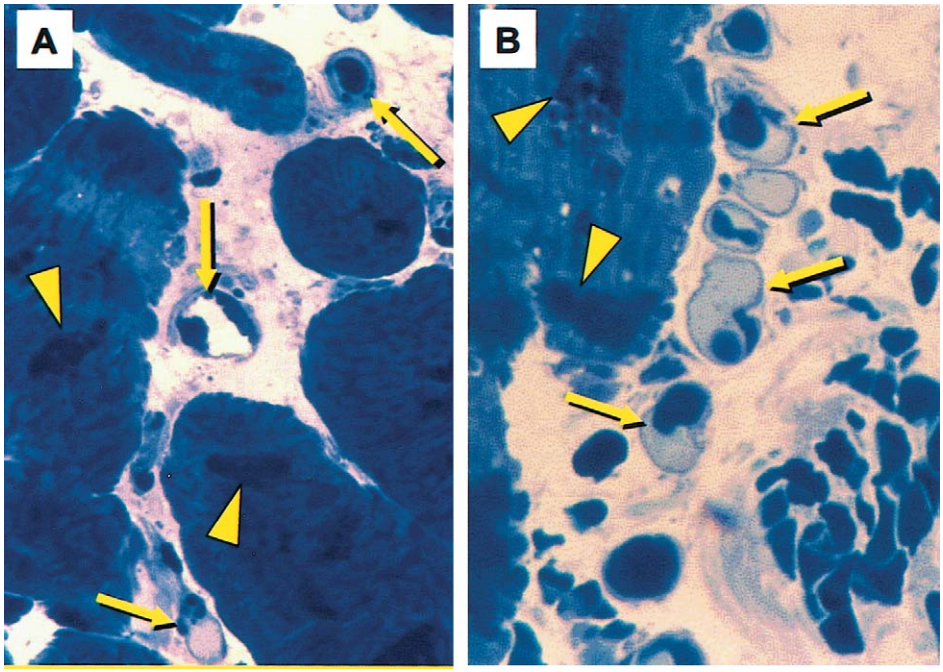

Figure 5 Photomicrographs of interstitial capillaries of the myocardium before (*A*) and after (*B*) treatment (methylene blue/azure II stain). Pretreatment (*A*), small-to-medium–sized glycosphingolipid inclusions were seen in the endothelium of small interstitial capillaries (*arrows;* score 2). After treatment (*B*), glycosphingolipid inclusions were cleared from the endothelium of small capillaries (*arrows*). The GL-3 inclusions in the cardiomyocytes (*arrowheads*) were less responsive to treatment. See text for details.

scopic evaluations, performed on a small number of samples, supported the findings from light microscopy.

Clinical Findings

Pre- and posttreatment EKGs, echocardiograms, and renal MRIs were unchanged. Patients anecdotally reported an increased ability to sweat and less fatigue. Pain was assessed by the Short Form McGill Pain Questionnaire. Compared to the pretreatment baseline results, the "overall pain" and "present pain intensity" scores were significantly improved after five infusions at all doses ($P = .03$ and $P = .004$, respectively). In addition, the SF-36 quality-of-life questionnaire indicated improvement posttreatment for three indices: bodily pain, general health, and vitality.

Safety Evaluation

Of the 15 patients, 13 completed all five r-hαGalA infusions, which were generally well tolerated. The most common adverse event was a transient mildly-to-moderately increased blood pressure during infusions, which did not require treatment and returned to normal during or immediately after infusion. There were no significant changes in blood indices or blood and urine chemistries. Patient 14 (group E), who had discontinued a 7-mo anticoagulant treatment for a deep vein thrombosis of a lower extremity prior to joining the study, complained of mild chest pain the day after he received his last r-hαGalA infusion. He was diagnosed with a pulmonary embolus, was retreated with anticoagulant therapy, and recovered without complication.

Of 15 patients, 8 developed IgG antibodies specific to r-hαGalA. Of these, the four who experienced symptoms compatible with hypersensitivity-type reactions had seroconverted. Two of these patients (patient 5, group B, and patient 7, group C), had symptoms suggestive of allergic reactions during infusion 4 and did not tolerate reinfusion, whereas the other two patients were successfully retreated. Importantly, despite this antibody response, mean pharmacokinetic values did not change between the first and fifth infusions for all patients studied (fig. 7).

Discussion

The primary finding of this phase 1/2 trial was that infused r-hαGalA safely and effectively cleared the accumulated GL-3 from endothelium of the liver, skin, heart, and kidney—major sites of pathology in classical Fabry disease. The demonstration that lysosomal glycosphingolipid accumulation in the microvasculature and other cell types was reversible provided "proof of principle" for enzyme-replacement therapy in this disease. Since

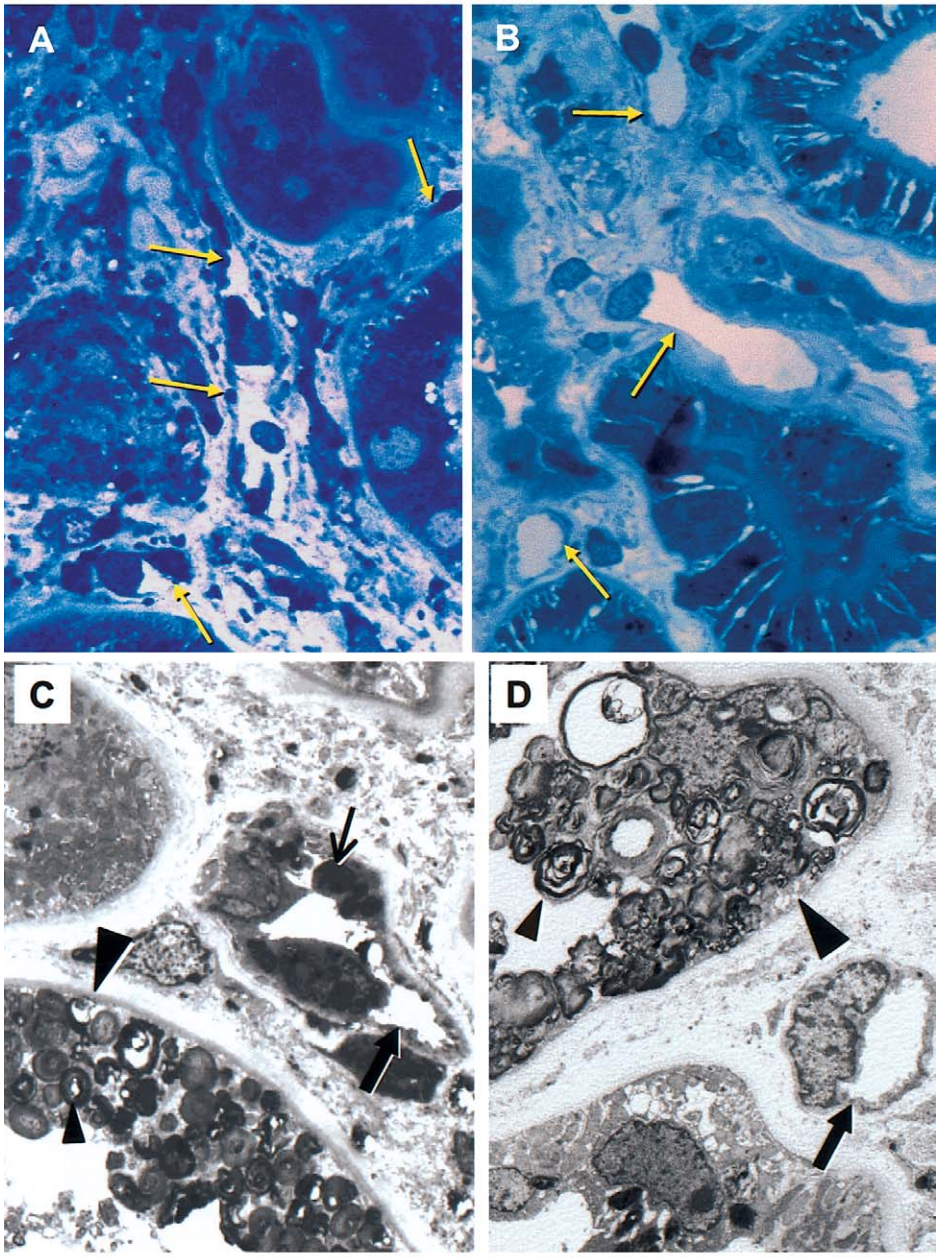

Figure 6 Light and electron micrographs of kidney pre- and posttreatment (methylene blue/azure II stain). *A* and *B*, Light microscopy of capillaries in the intertubular interstitium. Before treatment (*A*), the capillary endothelium (*arrows*) is heavily laden with glycosphingolipid inclusions, some impinging on the lumen (score 3). After treatment (*B*), most of the capillaries (*arrows*) have been cleared of glycosphingolipid inclusions (score 0). *C* and *D*, Electron micrographs of kidney cortex with examples of an intertubular capillary (*arrow*) and neighboring distal convoluted tubule (*arrowhead*). Before treatment (*C*), numerous electron-dense glycosphingolipid inclusions are seen in the capillary endothelium (*small arrow*). In the adjacent distal convoluted tubule, the epithelium is heavily packed with numerous electron-dense lamellar lysosomal inclusions (*small arrowhead*). After treatment (*D*), the endothelium of a small capillary (*arrow*) has no evidence of glycosphingolipid inclusions. In the adjacent distal convoluted tubule (*arrowhead*), the number and distribution of lysosomal inclusions appear similar; however, the lamellar architecture of the individual lysosomes appears less tightly organized (*small arrowhead*), suggesting enzymatic hydrolysis of the accumulated GL-3.

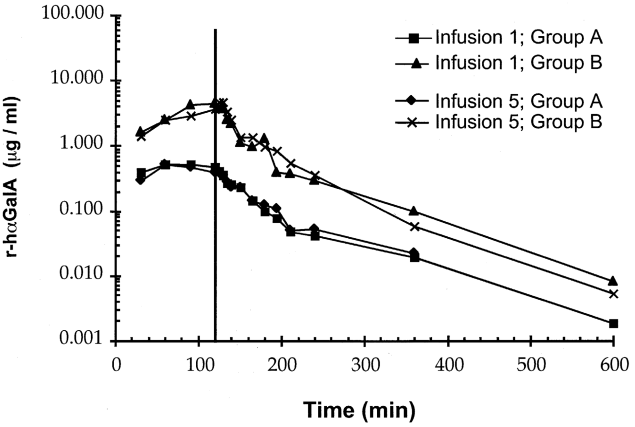

Figure 7 Comparison of the pharmacokinetics of r-hαGalA for infusions 1 and 5. Comparison of mean concentration-time data for groups A and B. R-hαGalA was infused over 120 min. Infusion 1: group A (●), group B (▲); infusion 5: group A (◆), group B (×). See text for details.

"cardiac variants" with Fabry disease lack microvascular glycosphingolipid accumulation and the major clinical manifestations of classically affected patients (Elleder et al. 1990; von Scheidt et al. 1991; Desnick et al. 2001), it is anticipated that the clearance of GL-3 from the microvasculature and other tissue sites of pathology should lead to significant physiologic and clinical improvement.

Beyond the microvascular GL-3 clearance, the glycosphingolipid tissue load and response to r-hαGalA treatment varied. Presumably, the different cellular glycosphingolipid levels reflected endogenous glycosphingolipid synthesis and cell turnover rates, whereas the differential clearance was a function of cellular and lysosomal enzyme uptake and stability. In the liver, which had the highest uptake of enzyme on the basis of the preclinical studies in "Fabry mice" (Ioannou et al. 2001), all dose regimens markedly reduced GL-3 levels; there was an 84% mean clearance of hepatic GL-3 by ELISA in patients with pre- and posttreatment biopsies (table 2). Morphologic examination revealed that the two principal hepatic reservoirs of glycosphingolipid—the endothelial cells of the sinusoids and the Kupffer cells—were almost totally cleared of glycosphingolipid inclusions. In comparison to other tissues studied, baseline endomyocardial GL-3 levels were the highest of those in all tissues studied, an order of magnitude greater than those in kidney (table 2). Histologic analysis revealed that the majority of GL-3 accumulation was in the cardiomyocytes and that the storage was not remarkably changed after five doses of r-hαGalA at 1 or 3 mg/kg. Similar results were documented by the ELISA determinations (table 2). Longer-term enzyme replacement presumably is required to reduce the substantial GL-3 accumulation in cardiomyocytes. Of note, preclinical studies in the "Fabry mouse" indicated that r-hαGalA activity was detectable in the heart when 3.0 mg/kg was infused (Ioannou et al. 2001).

Although the number of paired pre- and posttreatment renal biopsies for histologic analysis was limited, all three vascular beds showed the same response to treatment, a prominent reduction in GL-3 content from the endothelium. Total renal GL-3 levels, determined by ELISA, in four of the five patients with pre- and postbiopsy data also revealed a mean 82% reduction after treatment. Because the total vascular GL-3 content is a relatively small component of the total renal GL-3 accumulation, and because the podocyte inclusions were unchanged, most of the GL-3 reduction must have been from the tubules, the only other major storage site. Taken together with the reduction in vascular endothelial GL-3 levels, these results suggest potential benefit for kidney function.

In general, the biochemical and histologic assessments indicated that GL-3 clearance was dose and tissue-dependent, analogous to the findings of r-hαGalA replacement in "Fabry mice" (Ioannou et al. 2001). The biweekly dose regimens proved to be more effective than the every 48 h regimens, the latter included to assess the effects of a rapid, high-dose schedule (i.e., a "loading dose"), similar to that used in the preclinical studies (Ioannou et al. 2001). It was reasoned that administration every 48 h would achieve the highest enzyme concentration in lysosomes and the greatest plasma and tissue GL-3 clearance, particularly since the tissue half-life of the enzyme in the "Fabry mouse" was 2–4 d. However, the biweekly regimens unexpectedly cleared more substrate, the 1- and 3-mg/kg doses being more effective than the 0.3-mg/kg dose. Although assessment of GL-3 clearance in heart and kidney was limited, because of the small number of optional paired biopsies from patients in groups C–E, the greatest clearance was observed in patients in group C, who received 3 mg/kg biweekly. In addition, there was a direct effect of dose on plasma GL-3 levels. For example, plasma GL-3 was cleared from the circulation after the first infusion in patients in the 1.0- and 3.0-mg/kg biweekly dosing groups (fig. 2), whereas plasma GL-3 levels in the 0.3-mg/kg dosing group decreased with each infusion, reaching their lowest levels at infusion 4 or 5. Of interest, GL-3 reaccumulation in the plasma and tissues of "Fabry mice" following a single r-hαGalA dose (3 mg/kg) suggest that the plasma GL-3 level might reflect the total body load of substrate (Ioannou et al. 2001). Analogously, the plasma GL-3 concentration may provide a noninvasive indicator of tissue GL-3 clearance in patients with Fabry disease.

Clinically, the patients reported decreased pain and an increased ability to sweat, both findings consistent

with GL-3 clearance from microvascular endothelial cells. Improvements in several quality-of-life measures also were noted. However, assessments of pain and quality of life require more rigorous evaluation in a larger, double-blind study, to minimize possible placebo effects.

This phase 1/2 clinical trial also evaluated the safety of r-hαGalA infusions. Although the enzyme infusions were generally well tolerated, it was expected that most patients would raise antibodies to r-hαGalA, since classically affected males with Fabry disease are cross-reactive immunological material–negative for the α-Gal A protein (Desnick et al. 2001). In fact, four patients had mild-to-moderate hypersensitivity-type reactions: two with transient fever and chills, one with hives, and one with tachycardia. Although they responded to symptomatic treatment, two of these four patients were unable to complete their fifth infusions. Immunologic studies revealed that six (67%) of the nine patients on the biweekly dosing schedule seroconverted after the second or third infusion, whereas two (33%) of six patients on the every-48-h regimens seroconverted after the fifth infusion (day 9). In all cases, seroconversion was an IgG response, and almost identical pharmacokinetic profiles at the first and last infusions for both biweekly (fig. 7) and every-48-h (data not shown) infusion schedules indicated that antibodies were not neutralizing. Also, urine chemistry, blood cytology, and tissue-histology results were not altered in response to adverse reactions associated with enzyme infusions. On the basis of these findings and of previous experience with management of enzyme infusions for Gaucher disease (Grabowski et al. 1998; Mistry 1999), pretreatment with antipyretics and antihistamines, as well as decreasing the rate of infusion, are recommended for subsequent studies.

The most common adverse event associated with enzyme administration was a mild, transient increase in blood pressure, which did not require medical intervention or prevent patients who entered the trial with hypertension from safely completing their infusions. Only two serious adverse events occurred, and of these only one, an allergic reaction, was attributable to r-hαGalA administration. The other serious adverse event was a pulmonary embolism in a patient who recently discontinued anticoagulation treatment for a previous deep vein thrombosis. Of the other recorded adverse events, none was attributed to enzyme administration; however, several were associated with biopsy procedures.

In summary, the phase 1/2 clinical trial of r-hαGalA replacement in classically affected patients with Fabry disease demonstrated that the infused enzyme generally was well tolerated and that the expected infusion reactions following seroconversion were mild and conservatively managed. This trial provided the "proof of principle" that enzyme replacement could reverse the GL-3 accumulation in key sites of pathology. These results also indicated that the clearance of GL-3 from tissue lysosomes was dose-dependent and that enzyme could reach and hydrolyze the accumulated GL-3 in lysosomes. Finally, these studies provide the basis for a phase 3 pivotal trial with a greater number of patients to further evaluate the safety and efficacy of r-hαGalA replacement in Fabry disease.

Acknowledgments

The authors express their appreciation to the patients who participated in this trial, to our study coordinators (Melissa Nunn, B.A., and Athena Palearis, R.N.); to our medical fellows (Patricia Ashton-Prolla, M.D., and Kamal Topaloglu, M.D.); to our physician consultants (Mark W. Babyatsky, M.D., Meir Shinnar, M.D., and Swan N. Thung, M.D.); to the nursing and support staff of the General Clinical Research Center at the Mount Sinai School of Medicine, New York; and to our collaborators at the Genzyme Corporation (Richard Moscicki, M.D.; Susan Richards, Ph.D.; P. K. Tandon, Ph.D.; and their respective staffs). This work was supported in part by grants from the National Institutes of Health, including a Merit Award (5 R37 DK34045), a grant (5 M01 RR00071) for the Mount Sinai General Clinical Research Center, a grant (5 P30 HD28822) for the Mount Sinai Child Health Research Center, and a research grant from the Genzyme Corporation.

Electronic-Database Information

The accession number and URL for data in this article are as follows:

Online Mendelian Inheritance in Man (OMIM), http://www.ncbi.nlm.nih.gov/Omim (for Fabry disease [MIM 301500])

References

Bishop DF, Calhoun DH, Bernstein HS, Hantzopoulos P, Quinn M, Desnick RJ (1986) Human α-galactosidase A: nucleotide sequence of a cDNA clone encoding the mature enzyme. Proc Natl Acad Sci USA 83:4859–4863

Brady RO, Tallman JF, Johnson WG, Gal AE, Leahy WR, Quirk JM, Dekaban AS (1973) Replacement therapy for inherited enzyme deficiency: use of purified ceramidetrihexosidase in Fabry's disease. N Engl J Med 289:9–14

Colombi A, Kostyal A, Bracher R, Gloor F, Mazzi R, Tholen H (1967) Angiokeratoma corporis diffusum: Fabry's disease. Helv Med Acta 34:67–83

Desnick RJ, Allen KY, Desnick SJ, Raman MK, Bernlohr RW, Krivit W (1973) Fabry's disease: enzymatic diagnosis of hemizygotes and heterozygotes: α-galactosidase activities in plasma, serum, urine, and leukocytes. J Lab Clin Med 81: 157–171

Desnick RJ, Dean KJ, Grabowski G, Bishop DF, Sweeley CC (1979) Enzyme therapy in Fabry disease: differential in vivo

plasma clearance and metabolic effectiveness of plasma and splenic α-galactosidase A isozymes. Proc Natl Acad Sci USA 76:5326–5330

——— (1980) Enzyme therapy XVII: metabolic and immunologic evaluation of α-galactosidase A replacement in Fabry disease. Birth Defects Orig Artic Ser 16:393–413

Desnick RJ, Ioannou YA, Eng CM (1995) α-galactosidase A deficiency: Fabry disease. In: Scriver CR, Beaudet AL, Sly WS, Valle D (eds) The metabolic and molecular bases of inherited diseases, 7th ed. McGraw-Hill, New York, pp 2741–2784

——— (2001) α-galactosidase A deficiency: Fabry disease. In: Scriver CR, Beaudet AL, Sly WS, Valle D, Kinzler KE, Vogelstein B (eds) The metabolic and molecular bases of inherited diseases, 8th ed. McGraw-Hill, New York, pp 3733–3774

Elleder M, Bradova V, Smid F, Budesinsky M, Harzer K, Kustermann-Kuhn B, Ledvinova J, Belohlavek, Kral V, Dorazilova V (1990) Cardiocyte storage and hypertrophy as a sole manifestation of Fabry's disease: report on a case simulating hypertrophic non-obstructive cardiomyopathy. Virchows Arch A Pathol Anat Histopathol 417:449–455

Eng CM, Resnick-Silverman LA, Niehaus DJ, Astrin KH, Desnick RJ (1993) Nature and frequency of mutations in the α-galactosidase A gene that cause Fabry disease. Am J Hum Genet 53:1186–1197

Grabowski GA, Leslie N, Wenstrup R (1998) Enzyme therapy for Gaucher disease: the first 5 years. Blood Rev 12:115–133

Ioannou YA, Bishop DF, Desnick RJ (1992) Overexpression of human α-galactosidase A results in its intracellular aggregation, crystallization in lysosomes and selective secretion. J Cell Biol 119:1137–1150

Ioannou YA, Zeidner KM, Gordon RE, Desnick RJ (2001) Fabry disease: preclinical studies demonstrate the effectiveness of α-galactosidase A replacement in enzyme-deficient mice. Am J Hum Genet 68:14–25

Mapes CA, Anderson RL, Sweeley CC, Desnick RJ, Krivit W (1970) Enzyme replacement in Fabry's disease, an inborn error of metabolism. Science 169:987–989

Matsuura F, Ohta M, Ioannou YA, Desnick RJ (1998) Human α-galactosidase A: characterization of the *N*-linked oligosaccharides on the intracellular and secreted glycoforms overexpressed by Chinese hamster ovary cells. Glycobiology 8:329–339

Melzack R (1987) The short-form McGill pain questionnaire. Pain 30:191–197

Mistry PK (1999) Gaucher's disease: a model for modern management of a genetic disease. J Hepatol 30:1–5

Schiffmann R, Murray GJ, Treco D, Daniel P, Sellos-Moura M, Myers M, Quirk JM, Zirzow GC, Borowski M, Loveday K, Anderson T, Gillespie F, Oliver KL, Jeffries NO, Doo E, Liang TJ, Kreps C, Gunter K, Frei K, Crutchfield K, Selden RF, Brady RO (2000) Infusion of α-galactosidase A reduces tissue globotriaosylceramide storage in patients with Fabry disease. Proc Natl Acad Sci USA 97:365–370

von Scheidt W, Eng CM, Fitzmaurice TF, Erdmann E, Hubner G, Olsen EG, Christomanou H, Kandolf R, Bishop DF, Desnick RJ (1991) An atypical variant of Fabry's disease with manifestations confined to the myocardium. N Engl J Med 324:395–399

Wang AM, Ioannou YA, Zeidner KM, Gotleb RW, Dikman S, Stewart CL, Desnick RJ (1996) Generation of a mouse model with α-galactosidase A deficiency. Am J Hum Genet Suppl 59:A208

Ware J, Snow K, Kosinski M, Gandek B (1997) SF-36 health survey manual and interpretation guide. The Health Institute, New England Medical Center, Boston

Zeidner K, Desnick R, Ioannou Y (1999) Quantitative determination of globotriaosylceramide by immunodetection of glycolipid-bound recombinant verotoxin B subunit. Anal Biochem 267:104–113